Hindawi
Geofluids
Volume 2017, Article ID 8916313, 9 pages
https://doi.org/10.1155/2017/8916313

WILEY | Hindawi

Research Article

Computational Flow Dynamic Simulation of Micro Flow Field Characteristics Drainage Device Used in the Process of Oil-Water Separation

Guangya Jin and Zhijian Liu

Department of Power Engineering, School of Energy, Power & Mechanical Engineering, North China Electric Power University, Baoding, Hebei 071003, China

Correspondence should be addressed to Zhijian Liu; zhijianliu@ncepu.edu.cn

Received 11 April 2017; Accepted 31 May 2017; Published 4 July 2017

Academic Editor: Zhien Zhang

Aqueous crude oil often contains large amounts of produced water and heavy sediment, which seriously threats the safety of crude oil storage and transportation. Therefore, the proper design of crude oil tank drainage device is prerequisite for efficient purification of aqueous crude oil. In this work, the composition and physicochemical properties of crude oil samples were tested under the actual conditions encountered. Based on these data, an appropriate crude oil tank drainage device was developed using the principle of floating ball and multiphase flow. In addition, the flow field characteristics in the device were simulated and the contours and streamtraces of velocity magnitude at different nine moments were obtained. Meanwhile, the improvement of flow field characteristics after the addition of grids in crude oil tank drainage device was validated. These findings provide insights into the development of effective selection methods and serve as important references for oil-water separation process.

1. Introduction

The purpose of developing oilfields is to gain oil and natural gas which have broad use value, high economic benefit, and stringent specification. But, almost every oilfield around the world has to go through the development phase of water cut, especially oilfields which take fast recovery rate or water injection mode. Therefore, the aqueous crude oil is ubiquitous in the development of oilfield [1, 2]. Besides, crude oil and water also carry and dissolve a large collection of salts when moving in the reservoir, such as sulfate, carbonate, and chloride including potassium chloride and sodium chloride. Therefore, fuel-air mixture often contains large amounts of produced water, sediment, and other heavy solids. On the other hand, content of water will increase in later development, and salts are mainly dissolved in the water. According to statistics, weight ratio of water to oil can even reach 10, solids may reach 1 wt%~1.5 wt%, and more than 90% of produced crude oil requires tedious purification drainage [3].

The composition and quality of aqueous crude oil can directly affect application potential, increase treatment processes and delivery power consumption, and cause corrosion of metallic conduit and equipment. In addition, heavy solids can do great physical damage to metallic conduit and equipment. Furthermore, the aqueous crude oil has a strong impact on oil refinery processes [1, 3]. Salts and heavy solids contained in crude oil are usually dissolved and suspended in the water. As it has been mentioned, crude oil drainage is a comprehensive process of purification.

In the past drainage works, people detected oil-water surface with probe, opened drain valve artificially, and waited on duty. This method of operation has a lot of disadvantages, such as low automaticity, high safety requirements, and indefinable working hours. When large-capacity storage tanks drain by gravity, most of the water regions far from valve at the bottom of the tanks are deemed to be dead zone and the upper area will be flow zone if the open degree of drain valve is overlarge. If this part of oil due to vortex motion remixes with water and drain, the drying pool and air of drain

Table 1: Density and viscosity of oil and produced water.

Sample	Test temp (°C)	Density (g/ml)	Viscosity (mPa·s)
Oil	33	0.830	7.64
Produced water	22	1.015	0.96

area will be polluted, and that will consequentially increase burden for sewage treatment. But if the open degree of drain valve is too small, the efficiency will be low and people will waste much time for watching on duty. Besides, it could leave people at risks of hydrogen sulfide poisoning. Therefore, it is essential to design a new reasonable safety drainage device.

Some automatic or semiautomatic drainage devices were designed and produced [4–7], but some factors restrict the popularization and application in dehydration field, such as complex system, low reliability, high cost, and safety hazard.

2. Methods

2.1. Design Process of Drainage Device. In development process of drainage device, it is necessary to test the composition and physicochemical properties of crude oil sample because the valve body materials, device capacity, scale inhibition properties, and anticlogging measures are required to be determined according to the actual conditions.

In this paper, several exposed cylindrical metal arched storage tanks which have capacities of 3500 m^3 and 4500 m^3 are mainly studied. Ambient temperatures of oil storage district range from −28 to 33 degrees centigrade; the crude oil contains small amount of silt sediment; and volume ratio of water to tank is usually about 2.5%. According to field sampling and dewatering until water cut of sample is below 0.5%, then testing gel point of sample used test method for gel point of crude oils (Standard, China, SY/T0541-2009) as a reference [8]. The results indicated that the gel point of sample is 18 degrees centigrade, and the density and viscosity of oil and produced water are tested as shown in Table 1.

Salts, water, and other materials are unavoidably contained in crude oil, salts are mainly ionized in the water, crude oil intermixes with water, and then a relatively stable emulsion is formed. This emulsion makes an electrochemical reaction with vessel walls in the process of manufacture, storage, and transportation that will lead to vessel corrosion and loss of service life [9]. Meanwhile, the emulsion also can be attached to vessel walls and formed dirt because of high viscosity. All of the above factors will reduce efficiency of equipment. The demulsification process of pretreatment techniques of crude oil is for the purpose of excellent salt removal at minimum cost and effectively aids dehydration of crude oil. Besides, composition and physicochemical properties of oil sample are tested in lab. The results of chemical properties show that content of paraffin is 12.16%, colloid is 18.87%, asphalt is 4.23%, and sulfur is less than 0.03%. The test results of emulsion lay a foundation for the development of drainage device.

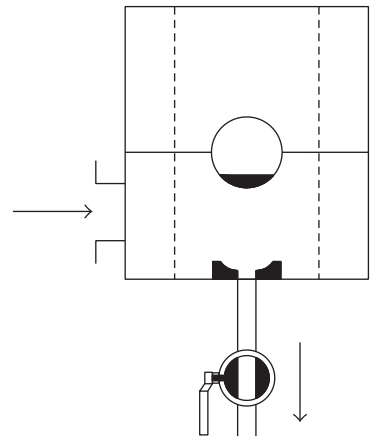

Figure 1: Schematic diagram of drainage device.

Schematic diagram of drainage device is shown in Figure 1. In the beginning, the floating ball is placed at the bottom of the device, and the water outlet is off. As the device starts to drain, the density of fluid is the same as water at the beginning, and the density of floating ball is less than fluid; thus the floating ball gradually moves upward and then makes the water outlet open. The flow rate is controlled by valve opening degree. As time goes on, the water level of oil tank continuously decreases and oil begins to enter the device for some time past. As the ratio of oil and water keeps on increasing, the density of mixture continuously decreases. The floating ball will gradually move downward and close the water outlet when the density of mixture is less than floating ball. Drainage will stop and the whole process is finished.

The density of floating ball is between crude oil and water, but the composition of crude oil is not unchangeable in the process of production. Therefore, it is necessary to increase or decrease the weight of floating ball for purpose that the density of floating ball is within a reasonable limit [10, 11]. Since the weight of floating ball has a great effect on drainage device, it should be watched closely at the change of oil quality and match the weight of floating ball in real applications.

2.2. Model Reconstruction. A large-capacity drainage device is calculated based on commercial computational fluid dynamic (CFD) code Fluent, core data is extracted, and necessary simplification is made through the preliminary design of device and relevant specification of the project. Three-dimensional model is established by using Unigraphics (UG) software, as shown in Figure 2. The drainage device is 600 mm high, the diameter of cylinder is 300 mm, the diameter of floating ball is 180 mm, and the diameter of inlet pipe is 150 mm and 50 mm for the outlet pipe. The dynamic layering model is used and number of dynamic mesh achieves 180,000. And unstructured grids are used too; the EquiSize Skew and EquiAngle Skew in detection are 0.52 and 0.43, respectively. It is indicated that the grids generated are simple, of high quality, and suitable [12].

In this paper, the realizable k-epsilon turbulence model was adopted, the volume of fluid model and second-order upwind model is appended, and the implicit unsteady

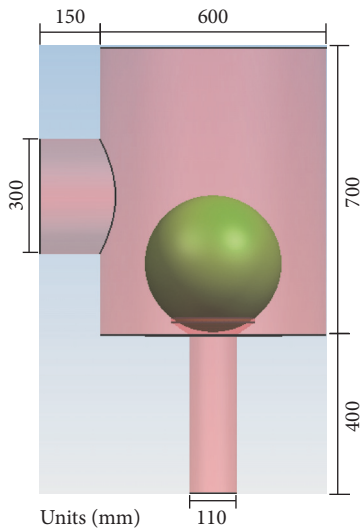

Figure 2: Three-dimensional model established by UG.

solution mode was adopted. The flow field characteristics were described by some calculated turbulent parameters like turbulent intensity, turbulent kinetic energy, turbulent scale, and turbulent dissipation rate apart from velocity and pressure.

2.3. CFD Method. The fluid in crude oil tank drainage device is assumed to be isothermal, adiabatic, and incompressible [12]. The approximate range of Reynolds number, one dimensionless parameter, is 850–2300 under different conditions in the model. Owing to the continuous change of the cross sections of this model and the velocity of the airflow, the Reynolds number changes incessantly. The highest Reynolds number can reach about 7200. Within the change range of the Reynolds number, the airflow in the crude oil tank drainage device model is turbulent. Based on the range of the Reynolds number, the standard k-ω model is chosen as the appropriate turbulence model in order to calculate the flow field characteristics of the inside crude oil tank drainage device more accurately.

The fundamental equations of the standard k-ω model are

$$\begin{aligned}
&\frac{\partial}{\partial t}(\rho k) + \frac{\partial}{\partial x_i}(\rho k u_i) = \frac{\partial}{\partial x_i}\left(\Gamma_k \frac{\partial k}{\partial x_i}\right) + G_k - Y_k + S_k \\
&\frac{\partial}{\partial t}(\rho \omega) + \frac{\partial}{\partial x_i}(\rho \omega u_i) \\
&\quad = \frac{\partial}{\partial x_j}\left(\Gamma_\omega \frac{\partial \omega}{\partial x_j}\right) + G_\omega - Y_\omega + S_\omega.
\end{aligned} \tag{1}$$

In these equations, G_k represents the turbulence kinetic energy generated by laminar velocity gradient. G_ω is generated by the ω equation; Γ_k and Γ_ω represent the diffusivities of k and ω, respectively; Y_k and Y_ω represent the turbulence generated by diffusion. S_k and S_ω are user-defined source terms.

This article uses the commercial software Ansys14 for the CFD calculation. Based on the finite volume method, the Ansys software owes the characteristics like good stability, wide scope of application, high precision, and so forth. The calculation process uses separate method and adopts the SIMPLE algorithm to couple the pressure and velocity. It belongs to one method of the pressure correction methods and is presented by Patankar and Spalding in 1972 [13]. The dispersion of G_k and ω adopts second-order upwind scheme.

The ICEM-CFD (Integrated Computer Engineering and Manufacturing code for Computational Fluid Dynamics) is used in grid division for this real model. Because the upper respiratory tracts model is real, the structure is extremely complex. So the grid division adopts the tetrahedral grid form of the unstructured grid. According to literature [14], this unstructured tetrahedral grid can well reflect the flow field of the respiratory tracts. It makes favorable qualities by proper regional compactness in the sections owing to large curvature. From the calculations of 400000, 700000, and 1050000 grid numbers, respectively, the 700000 grid numbers can satisfy the calculation requirements and reflect the characteristics of flow field better. The convergence criteria are defined as 10^{-5} here.

3. Results and Discussion

The density of fluid was controlled by User-Defined Function (UDF), and the area and numbers of dynamic grid generations continually changed over time. Based on positions of floating ball at different moments, the whole process was divided into nine moving stages (T1–T9) during all this movement for the purpose of studying flow field of drainage device. Contours of velocity magnitude and streamtraces were shown in Figures 5 and 6, respectively.

It was shown in Figure 3 that the floating ball moved upward from T1 moment to T4 moment and the gap at the bottom of the floating ball kept on increasing, because the outlet flow was always less than the inlet flow and the density of floating ball was less than current fluid. For the movement of the floating ball, the maximum velocities were on a declining curve. From T5 to T7, typical pipe flow characteristics were shown and the maximum velocities appeared in the central position of pipe and maintained stability. At these moments, the outlet flow was basically in accordance with the inlet flow and the device enjoyed optimal draining condition. As the density of fluid decreased continuously from T8 moment to T9 moment, the floating ball moved downward under gravity. And the gap at the bottom of the floating ball kept on decreasing, which leads to slight increase of the maximum velocity.

The result in Figure 4 showed that there were always vortexes of which the position and scope differed greatly at the lower left of the device during movement of the floating ball; meanwhile the streamtraces were also widely variable. In contrast to results from T7 to T9 in Figures 5 and 6, the contours of velocity magnitude were similar at the same position during movement of the floating ball, but the streamtraces were quite different, which indicated

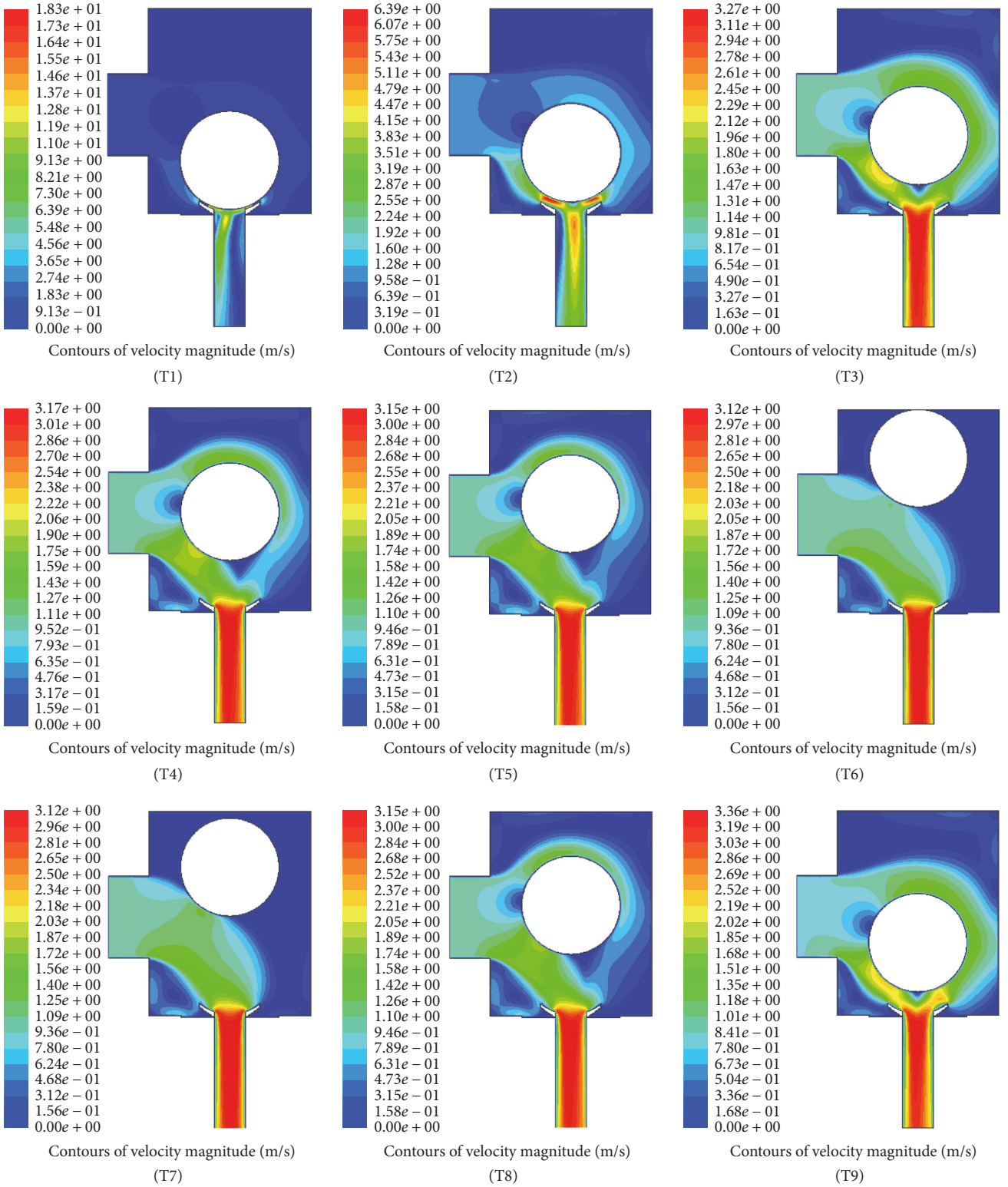

Figure 3: Contours of velocity magnitude during movement of floating ball.

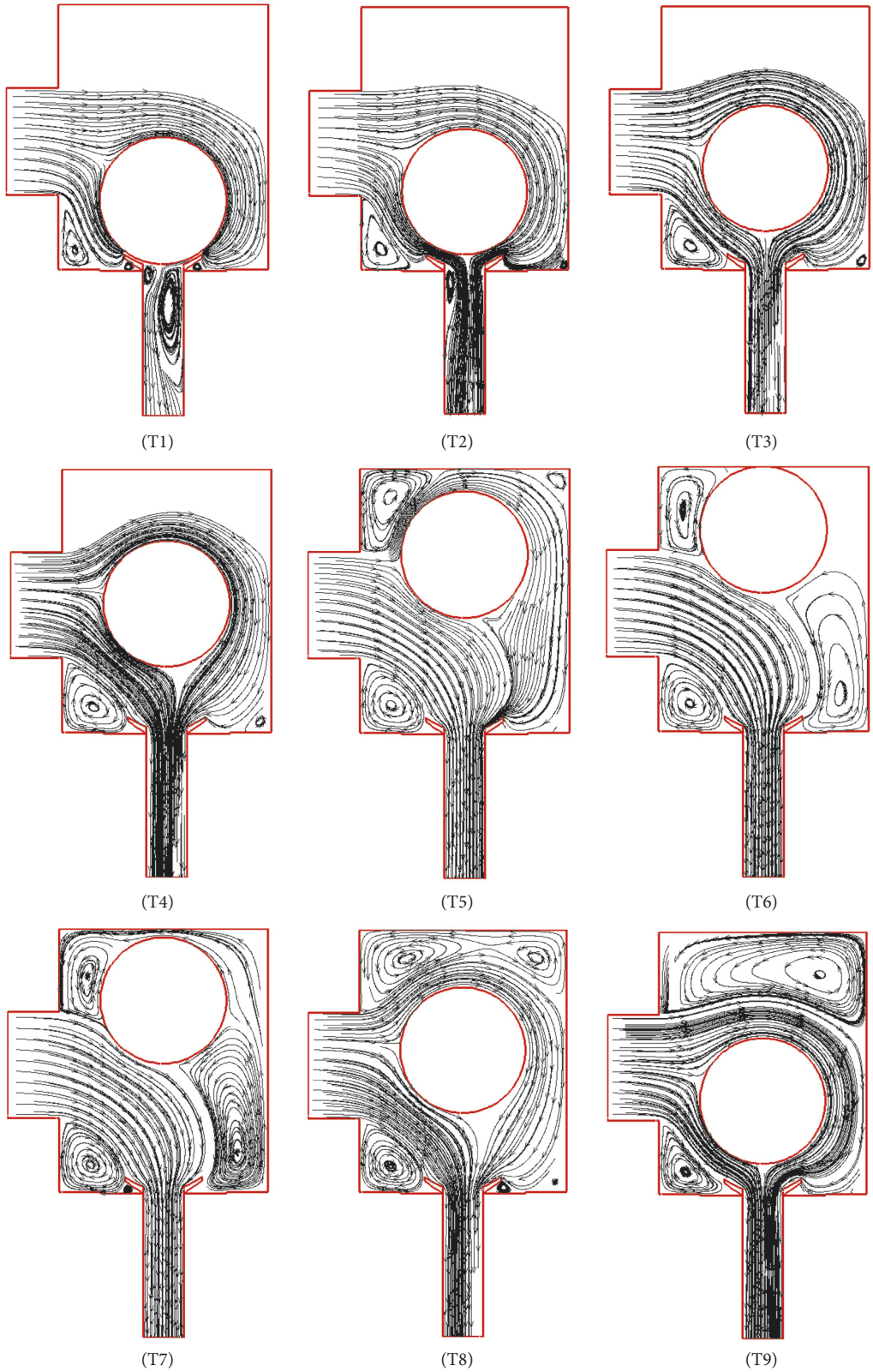

Figure 4: Streamtraces during movement of the floating ball.

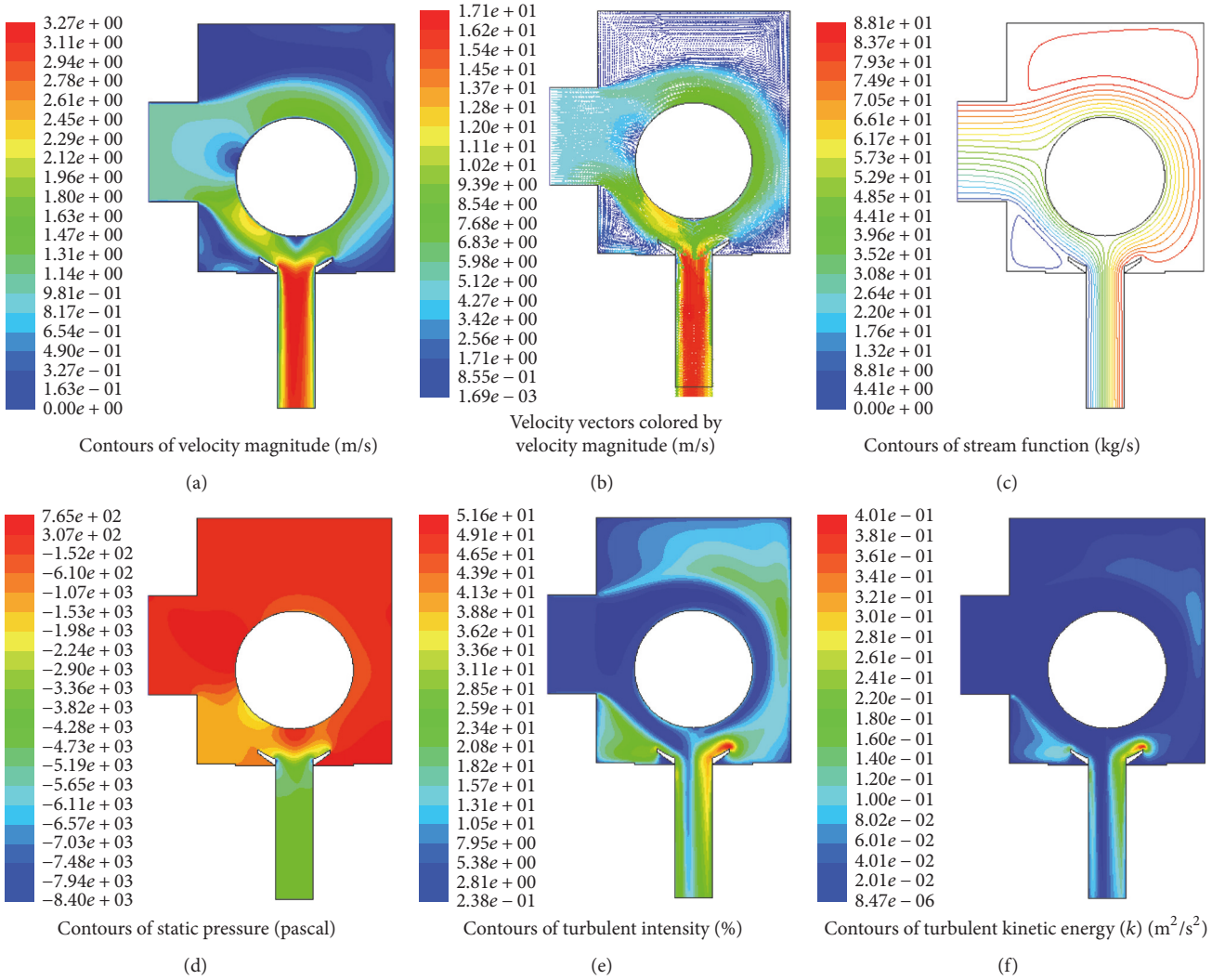

FIGURE 5: (a) Contours of velocity magnitude; (b) contours of velocity vector; (c) contours of stream function; (d) contours of static pressure; (e) contours of turbulent intensity; (f) contours of turbulent kinetic energy in drainage device at T3 moment.

that the flow field characteristics had big differences during movement of the floating ball.

3.1. Analysis of Interior Flow Field Characteristics. Confined to the length of the thesis, only flow field characteristics at T3 moment and T6 moment were analyzed. Contours of velocity magnitude (a), velocity vector (b), stream function (c), static pressure (d), turbulent intensity (e), and turbulent kinetic energy (f) in drainage device at T3 moment were described, as shown in Figure 5. At this moment, the floating ball had just reached the lower mid position of liquid inlet, and the gap at the bottom of the floating ball kept on increasing. The flushing action of influent liquid led to uneven force of the floating ball, but flow irregularity turned to be weak. As shown in Figure 4, the flow field on left and right sides of floating ball displayed an asymmetric distribution, and the left side showed an area of lower velocity. The flow field on the right side was uniformly distributed, and velocity increased from device walls to surface of floating ball. As shown in Figure 5(c), the lower left of device formed vortex because of the flushing action of influent liquid and retardation in the local scope. The flow field on upside of floating ball maintained stability, and the maximum velocity appeared in the central position of drainpipe.

As shown in Figure 5(d), the static pressure underneath the floating ball had risen to the same level as the upside of the floating ball. Surprisingly, the static pressure in the drainpipe was much lower and well distributed. Figures 5(e) and 5(f) showed that the maximum turbulent intensity, at a value of 5.16, existed at the lower right of the floating ball and the right side in the drainpipe. The value of maximum turbulent kinetic energy was 4 m^2/s^2. This situation may result from the fact that the floating ball was almost at the opposite side to the water inlet, which promoted the formation of disturbance. Scrutinizing the turbulent intensity and turbulent kinetic energy revealed the variation of the former is more dramatic than the latter.

Contours of velocity magnitude (a), velocity vector (b), stream function (c), static pressure (d), turbulent intensity (e), and turbulent kinetic energy (f) in drainage device at T6

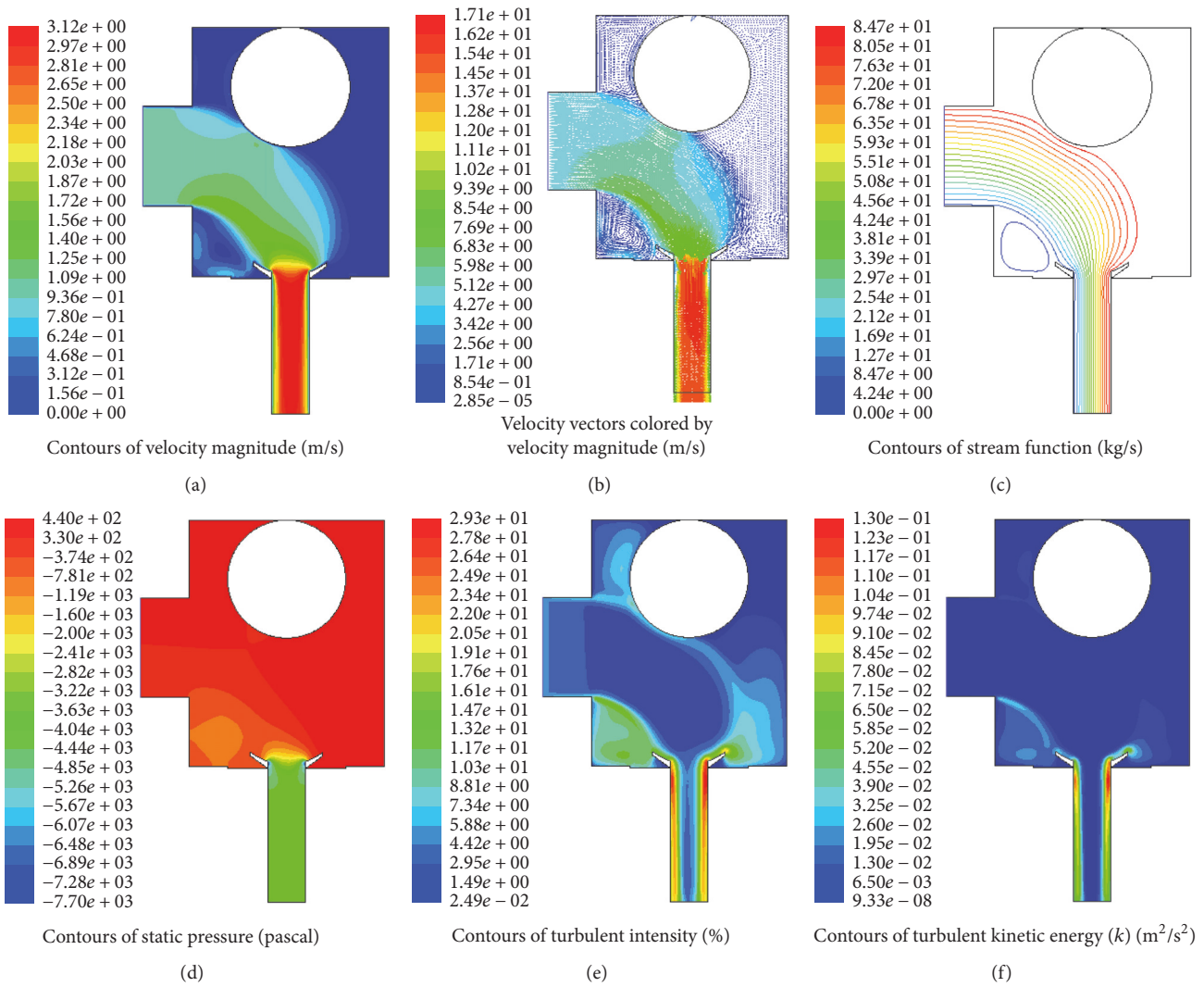

FIGURE 6: (a) Contours of velocity magnitude; (b) contours of velocity vector; (c) contours of stream function; (d) contours of static pressure; (e) contours of turbulent intensity; (f) contours of turbulent kinetic energy in drainage device at T6 moment.

moment were described, as shown in Figure 6. Figures 6(a), 6(b), and 6(c) showed that the velocity of the lower left side of the floating ball was bigger than one of the right side which almost appeared in static state. Besides, velocity distribution was obviously asymmetrical, typical pipe flow characteristics were shown, and the maximum velocity which achieved 3.12 m/s appeared in the central position of drainpipe.

It was shown in Figure 3 (T6), Figure 4 (T6), and Figure 6(c) that the flow field of upper right side was almost static state. Scrutinizing the postprocessing results by Tecplot and Fluent software, respectively, revealed the variation of the former shows better details of flow field characteristics such as detailed distribution, direction, and distance of streamlines, but the latter is better at fast output of streamlines.

As shown in Figure 7(d), the static pressure of lower left side of the device was almost the same with the upper side, and the static pressure of the inlet position was lower because of dynamic pressure. Contours of turbulent intensity (e) was similar with ones of turbulent kinetic energy (f); both of them showed that higher turbulent intensity and turbulent kinetic energy appeared at the lower left side and lower right side of the floating ball's bottom in the device, and the maximum value appeared at both sides of the top in the drainpipe. The turbulent intensity at the inlet position of the device was lower because there was larger inlet as well as smaller outlet in the device [15]. At this moment, turbulence of fluid was lower and it was beneficial to drain.

3.2. Effects on Installation of Grids. Installation of grids in the device can be used to enhance stability of floating ball, make the inlet water well distributed, and decrease the flushing action to floating ball. Besides, the grids could also decrease the turbulent intensity of the flow field in the device, cut the stagnant area of water in drainage process, and guarantee the device safe, stable, and highly efficient operation. The grids installed in device were 390 mm high, and the diameter of cylinder was 248 mm, the size of circular mesh was 6 mm, and thickness was 2 mm. The flow field characteristics

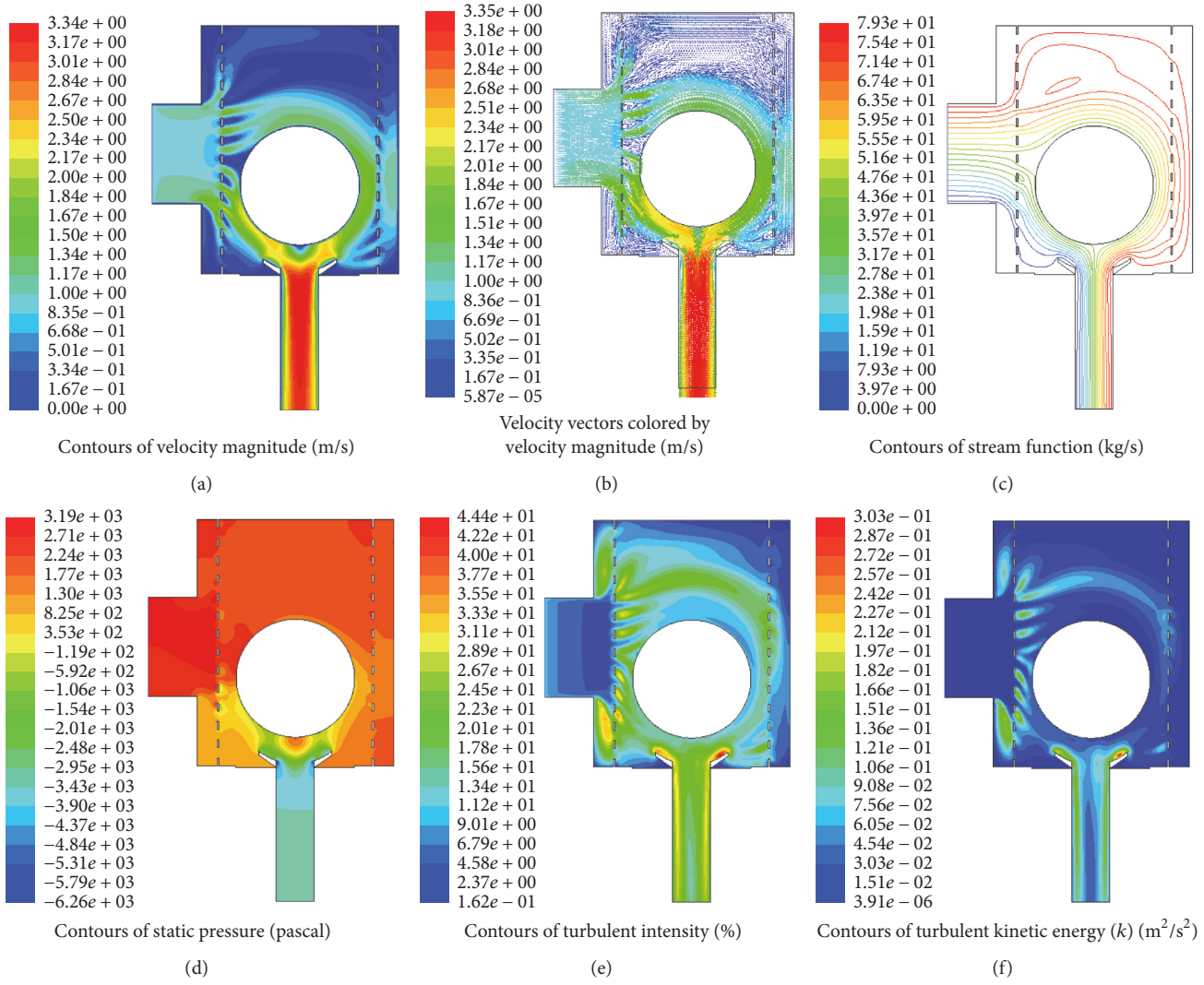

FIGURE 7: (a) Contours of velocity magnitude; (b) contours of velocity vector; (c) contours of stream function; (d) contours of static pressure; (e) contours of turbulent intensity; (f) contours of turbulent kinetic energy after installation of grids at T3 moment.

after installation of grids at T3 moment were shown in Figure 7.

In contrast to contours of velocity magnitude (a) and velocity vector (b) before (Figure 7) and after (Figure 7) installation of grids in the device at T3 moment, it was shown that the velocity of liquid at the position of inlet was distributed in a holistic uniform manner, various parts in the device can be faster filled with liquid, and it was beneficial to higher efficiency drainage after the installation of grids. Contours of stream function (c) showed that the formed vortex was significantly reduced and the streamline was more uniform. The results suggested that the flushing action of liquid turned to be weak. Figure 7(d) indicated that the static pressure on both sides was uniform symmetric distribution and the stability was enhanced as well as a lower head loss characteristic.

In contrast to contours of turbulence intensity (e) and turbulent kinetic energy (f), it was shown that the turbulence intensities varied widely before and after the installation of grids, and obviously the latter was distributed in a holistic uniform manner. Meanwhile, turbulence of the drainage device was lower. It could improve the characteristics of flow field by adding the grids, which was also mentioned in other literatures [16–18].

4. Conclusions

The following conclusions could be drawn as follows:

(1) It is extremely important to test the physicochemical properties of crude oil sample for rational design of drainage device and accurate simulation of flow field characteristics.

(2) The flow field characteristics of drainage device, including pressure, velocity, and turbulent intensity, are obtained by numerical simulation method, which could reflect the validity of drainage effectiveness.

(3) Installation of grids could significantly optimize the flow field characteristics and, furthermore, improve the effectiveness of drainage and oil-water separation process.

(4) The analysis on the parameters such as velocity magnitude, vector, and stream function is conductive to drainage device design modification.

These findings provide insights into the development of effective selection methods and serve as important references for oil-water separation process.

Conflicts of Interest

The authors declare no conflicts of interest.

Authors' Contributions

In this research work, all the authors were involved in the CFD simulation, results analysis and discussion, and manuscript preparation.

Acknowledgments

This work was supported by the Research Funds of Key Laboratory of Heating and Air Conditioning, The Education Department of Henan Province (no. 2017HAC105), and the Fundamental Research Funds for the Central Universities (2017MS119).

References

[1] J. Jing, N. Duan, K. Dai et al., "Investigation on drag characteristics of heavy oil flowing through horizontal pipe under the action of aqueous foam," *Journal of Petroleum Science and Engineering*, vol. 124, pp. 83–93, 2014.

[2] F. J. Argüelles-Vivas and T. Babadagli, "Drainage type oil and heavy-oil displacement in circular capillary tubes: two-and three-phase flow characteristics and residual oil saturation development in the form of film at different temperatures," *Journal of Petroleum Science and Engineering*, vol. 118, pp. 61–73, 2014.

[3] J.-E. Forero, O.-P. Ortíz, F.-A. Nariño, J. Díaz, and H. Peña, "Design and development of a high efficiency tank for crude oil dehydration," *Ciencia, Tecnología y Futuro*, vol. 3, no. 4, pp. 185–199, 2008.

[4] W. Wang, J. Gong, and P. Angeli, "Investigation on heavy crude-water two phase flow and related flow characteristics," *International Journal of Multiphase Flow*, vol. 37, no. 9, pp. 1156–1164, 2011.

[5] Q. Li, F. B. Li, and X. Y. Su, "Research on a new type of device of laminar water draining with no external force," *Advanced Materials Research*, vol. 201-203, pp. 2238–2241, 2011.

[6] Y. Q. Xu, Z. C. Guan, Y. W. Liu, L. C. Xuan, H. N. Zhang, and C. B. Xu, "Structural optimization of downhole float valve via computational fluid dynamics," *Engineering Failure Analysis*, vol. 44, pp. 85–94, 2014.

[7] Y. Shi, F. Tang, and X. Wang, "Simulation research on micro-avity flow field characteristics of liquid floating rotor gyro," *Key Engineering Materials*, vol. 562-565, pp. 490–495, 2013.

[8] Test method for gel point of crude oils. SY/T0541-2009, Standard, China, 2009.

[9] I. G. Harpur, N. J. Wayth, A. G. Bailey, M. T. Thew, T. J. Williams, and O. Urdahl, "Destabilisation of water-in-oil emulsions under the influence of an A.C. electric field: experimental assessment of performance," *Journal of Electrostatics*, vol. 40, pp. 135–140, 1997.

[10] K. Mahdi, R. Gheshlaghi, G. Zahedi, and A. Lohi, "Characterization and modeling of a crude oil desalting plant by a statistically designed approach," *Journal of Petroleum Science and Engineering*, vol. 61, no. 2-4, pp. 116–123, 2008.

[11] J. Gong, Y. Zhang, L. Liao, J. Duan, P. Wang, and J. Zhou, "Wax deposition in the oil/gas two-phase flow for a horizontal pipe," *Energy and Fuels*, vol. 25, no. 4, pp. 1624–1632, 2011.

[12] L. A. Dillard, H. I. Essaid, and W. N. Herkelrath, "Multiphase flow modeling of a crude-oil spill site with a bimodal permeability distribution," *Water Resources Research*, vol. 33, no. 7, pp. 1617–1632, 1997.

[13] S. V. Patankar and D. B. Spalding, "A calculation procedure for heat, mass and momentum transfer in three-dimensional parabolic flows," *International Journal of Heat and Mass Transfer*, vol. 15, no. 10, pp. 1787–1806, 1972.

[14] N. Yang, W. Wang, W. Ge, and J. Li, "CFD simulation of concurrent-up gas-solid flow in circulating fluidized beds with structure-dependent drag coefficient," *Chemical Engineering Journal*, vol. 96, no. 1-3, pp. 71–80, 2003.

[15] Z. Zhang, Y. Yan, D. A. Wood et al., "Influence of the membrane module geometry on so2 removal: a numerical study," *Industrial and Engineering Chemistry Research*, vol. 54, no. 46, pp. 11619–11627, 2015.

[16] S. Eiamsa-ard and P. Promvonge, "Numerical simulation of flow field and temperature separation in a vortex tube," *International Communications in Heat and Mass Transfer*, vol. 35, no. 8, pp. 937–947, 2008.

[17] Z. Han, B. H. Dennis, and G. S. Dulikravich, "Simultaneous prediction of external flow-field and temperature in internally cooled 3-D turbine blade material," in *Proceedings of the ASME Turbo Expo 2000: Power for Land, Sea, and Air*, American Society of Mechanical Engineers, Munich, Germany, 2000.

[18] C. M. Rhie and W. L. Chow, "Numerical study of the turbulent flow past an airfoil with trailing edge separation," *AIAA Journal*, vol. 21, no. 11, pp. 1525–1532, 1983.